

Variability in the South Atlantic Anticyclone and the Atlantic Niño Mode*

JOKE F. LÜBBECKE⁺

National Oceanic and Atmospheric Administration/Pacific Marine Environmental Laboratory, Seattle, Washington

NATALIE J. BURLS

Department of Geology and Geophysics, Yale University, New Haven, Connecticut

CHRIS J. C. REASON

Department of Oceanography, University of Cape Town, Cape Town, South Africa

MICHAEL J. MCPHADEN

National Oceanic and Atmospheric Administration/Pacific Marine Environmental Laboratory, Seattle, Washington

(Manuscript received 13 March 2014, in final form 30 June 2014)

ABSTRACT

Previous studies have argued that the strength of the South Atlantic subtropical high pressure system, referred to as the South Atlantic anticyclone (SAA), modulates sea surface temperature (SST) anomalies in the eastern equatorial Atlantic. Using ocean and atmosphere reanalysis products, it is shown here that the strength of the SAA from February to May impacts the timing of the cold tongue onset and the intensity of its development in the eastern equatorial Atlantic via anomalous tropical wind power. This modulation in the timing and amplitude of seasonal cold tongue development manifests itself via SST anomalies peaking between June and August. The timing and impact of this connection is not completely symmetric for warm and cold events. For cold events, an anomalously strong SAA in February and March leads to positive wind power anomalies from February to June resulting in an early cold tongue onset and subsequent cold SST anomalies in June and July. For warm events, the anomalously weak SAA persists until May, generating negative wind power anomalies that lead to a late cold tongue onset as well as a suppression of the cold tongue development and associated warm SST anomalies. Mechanisms by which SAA-induced wind power variations south of the equator influence eastern equatorial Atlantic SST are discussed, including ocean adjustment via Rossby and Kelvin wave propagation, meridional advection, and local intraseasonal wind variations.

1. Introduction

Sea surface temperature (SST) variations in the tropical oceans have a large effect on the marine ecosystem and rainfall variability over adjacent land regions and thus lead to large socioeconomic impacts. It is therefore

of high importance to understand the mechanisms that generate these SST anomalies in order to improve their predictability.

Unlike in the tropical Pacific where the El Niño–Southern Oscillation (ENSO) is the dominant mode of variability, variations of comparable magnitude on a range of time scales interact in the tropical Atlantic. The seasonal development of the cold tongue in boreal summer, on and slightly south of the equator between approximately 20°W and 0°, results in a large seasonal cycle in eastern equatorial Atlantic (EEA) SST. Interannual SST anomalies in this region (Fig. 1a) are associated with the Atlantic zonal mode. Also referred to as the Atlantic Niño mode, events constituting of strong warm (cold) interannual SST anomalies are called Atlantic Niño (Niña) events. Their occurrence is phase locked to June–August

* Pacific Marine Environmental Laboratory Publication Number 4140.

⁺ Current affiliation: GEOMAR Helmholtz Centre for Ocean Research Kiel, Kiel, Germany.

Corresponding author address: Joke F. Lübbecke, GEOMAR Helmholtz Centre for Ocean Research Kiel, Düsternbrooker Weg 20, 24105 Kiel, Germany.
E-mail: jluebbecke@geomar.de

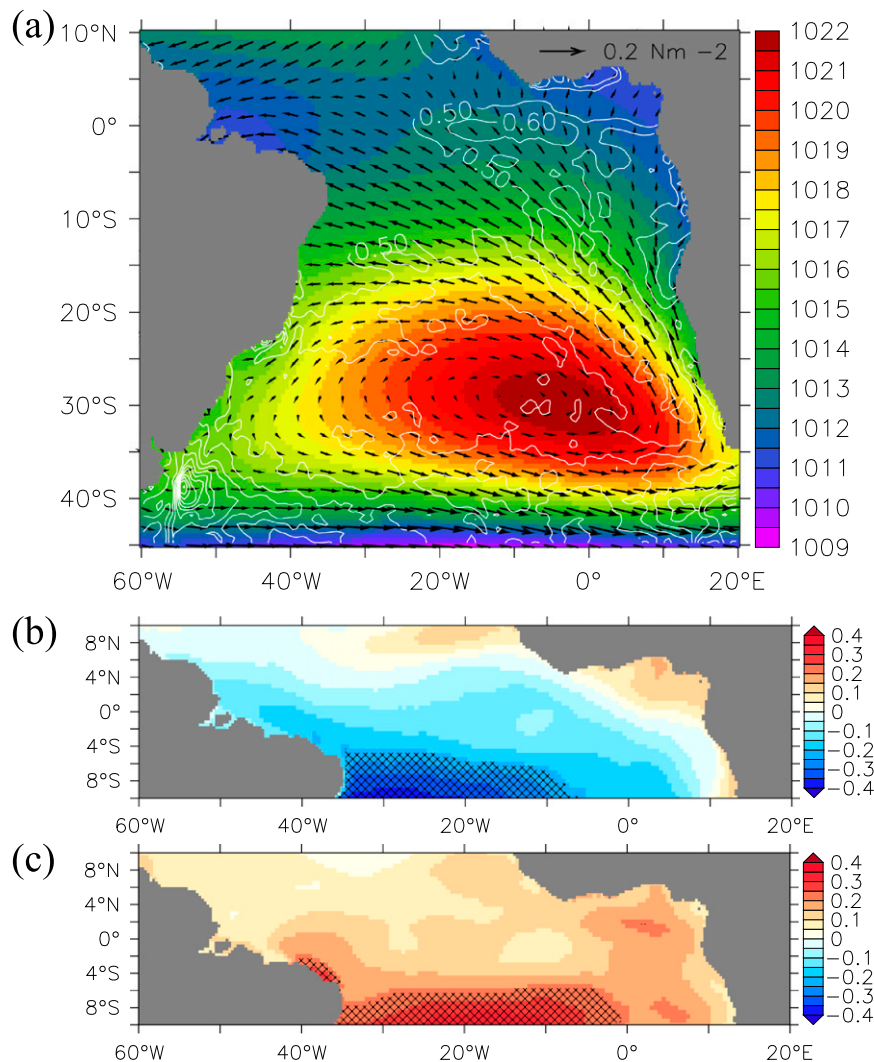


FIG. 1. (a) Regional overview with color shading showing the mean sea level pressure (hPa) from ERA-Interim (1980–2008). The superimposed black vectors and white contours show the mean ERA-Interim (1980–2008) wind stress field (N m^{-2}) and standard deviation associated with SODA2.2.4 (1980–2008) interannual SST anomalies ($^{\circ}\text{C}$), respectively. (b),(c) Correlation between an index representing interannual anomalies in the strength of the SAA (defined in section 2 and referred to throughout the paper as the SAA index) and (b) zonal and (c) meridional wind stress in the tropical Atlantic from ERA-Interim for 1980–2008 at zero lag. Hatching indicates values that are statistically significant at the 95% level.

(JJA), when the thermocline is shallow and upwelling is at its maximum (Keenlyside and Latif 2007). From an energetics perspective, Burls et al. (2012) showed that interannual SST anomalies in the EEA can be understood as modulations of a seasonally active thermocline mode. Modulations in the timing and intensity of the seasonally excited Bjerknes feedback between April and July are the primary cause of anomalous SST associated with the Atlantic Niño mode. An amplification (suppression) of the seasonal cycle leads to a cold (warm) anomaly in JJA. In addition to variations in

amplitude, a shift in the timing of the cold tongue onset can also result in an SST anomaly (Marin et al. 2009; Burls et al. 2012). Caniaux et al. (2011) investigated the variability in the onset, spatial extent, and temperature of the cold tongue for the 26 individual years between 1982 and 2007. They found that the timing of the cold tongue formation between March and mid-June depends on the timing of the seasonal intensification of the southeasterly trades that is in turn associated with the South Atlantic subtropical high pressure system, referred to as the South Atlantic anticyclone (SAA). A

connection between the strength of the SAA and SST anomalies in the southeastern tropical Atlantic has also been described by Lübbecke et al. (2010). They found a weakening of the SAA in February and March prior to Atlantic warm events in JJA. Also, Richter et al. (2010) highlighted the importance of a weakening of the SAA in the development of warm events off Angola and in the EEA. Hu et al. (2013) described a tilt mode in the equatorial Atlantic Ocean that represents an equatorial balanced response between the zonal thermocline slope and zonal wind variations. They found that this mode is triggered from the south by fluctuations in the SAA.

Despite the many studies that link the SAA and SST anomalies in the southeastern tropical Atlantic, the exact causal relationship remains unclear. Changes in the strength of the SAA are expected to be associated with variability in the southeasterly trade winds and meridional winds along the southwestern coast of Africa. While the latter impacts coastal upwelling, changes in the trade winds in the western equatorial Atlantic can excite eastward-propagating equatorial Kelvin waves that are associated with vertical displacement of the thermocline, thus leading to SST anomalies in the east. However, the correlation between the SAA and wind stress anomalies in the western and central equatorial Atlantic is actually rather low [shown for the European Centre for Medium-Range Weather Forecasts Interim Re-Analysis (ERA-Interim) in Figs. 1b,c; very similar results are obtained if other reanalysis products are used].

Following Burls et al. (2012), here we analyze the connection between the SAA and EEA SST anomalies from an energetics perspective, focusing on the role of anomalous wind power. Burls et al. (2012) showed that, as the primary source of anomalous tropical Atlantic available potential energy, anomalous wind power over the tropical Atlantic is a potential predictor for Atlantic Niño and Niña events. Tropical Atlantic wind power values between January and July are typically anomalously large during cold event years while they are anomalously weak between April and July for warm event years. Based on the results by Lübbecke et al. (2010), they suggested that SAA variability might be an important source of anomalous tropical Atlantic wind power.

The main questions that we want to address in this study are as follows. 1) What is the role of the SAA in exciting SST variability in the EEA and 2) is variability in the strength of the SAA mainly influencing the timing of the cold tongue onset, via an early/late onset of the trades, or is it also forcing changes in the intensity of the seasonal cycle of SST in the cold tongue region?

The remainder of this study is organized as follows. In section 2, the datasets used in this study and the wind power calculation are described. Section 3 presents the

results on the connection between the SAA and EEA SST variability. In section 4 we discuss possible mechanisms by which changes in wind power south of equator impact EEA SST and a potential connection to ENSO. The results are summarized in section 5.

2. Data and methods

Monthly fields of wind stress, SST, and ocean velocity for the time period 1980–2008 are taken from the Simple Ocean Data Assimilation (SODA) reanalysis product in version 2.2.4 (SODA2.2.4; Carton and Giese 2008), which is forced with Twentieth Century Reanalysis, version 2 (20CRv2) surface winds (Compo et al. 2011), and from the National Centers for Environmental Prediction–U.S. Department of Energy (NCEP–DOE) Atmospheric Model Intercomparison Project II (AMIP-II) reanalysis (NCEP-2) forced Global Ocean Data Analysis System (GODAS) analysis product (Behringer and Xue 2004). These products have 40 vertical levels and horizontal resolutions of 0.25° and 1° , respectively. For sea level pressure (SLP), we use ERA-Interim with a spectral T255 (corresponding to about 0.7°) horizontal resolution (Dee et al. 2011) and the NCEP-2 reanalysis product, provided by the National Oceanic and Atmospheric Administration (NOAA)/Office of Oceanic and Atmospheric Research/Earth System Research Laboratory/Physical Sciences Division (NOAA/OAR/ESRL/PSD), Boulder, Colorado, at a spatial resolution of 2.5° (Kanamitsu et al. 2002). Interannual anomalies are calculated by subtracting a repeated mean seasonal cycle from the full time series. All time series are detrended.

To estimate the strength of the SAA, an index is calculated by averaging SLP anomalies over 40° – 10° S, 40° – 10° W. As a measure for SST variability in the EEA, SST anomalies are averaged over the Atlantic 3 region (Atl3: 20° W– 0° , 3° S– 3° N). As illustrated in Fig. 1a by the closed 0.6° C white contour situated in the eastern equatorial Atlantic, the Atl3 region corresponds with the region of maximum equatorial interannual SST variability. As the region of highest zero lag correlation with Atl3 SST, western equatorial Atlantic (WEA) wind stress is averaged over 2° S– 2° N, 40° – 10° W.

SST anomalies in the EEA can largely be regarded as the surface expressions of upper-ocean energy changes. As seen interannually in the Pacific (Goddard and Philander 2000; Fedorov et al. 2003; Fedorov 2007; Brown and Fedorov 2010), the eastern basin SST is well correlated with the available potential energy of the basin as it succinctly quantifies changes in the zonal slope of the thermocline. Atl3 SST is well correlated with the available potential energy of the tropical Atlantic (8° S– 8° N, 60° W– 15° E; 0–400 m) both seasonally (Burls et al. 2011) and

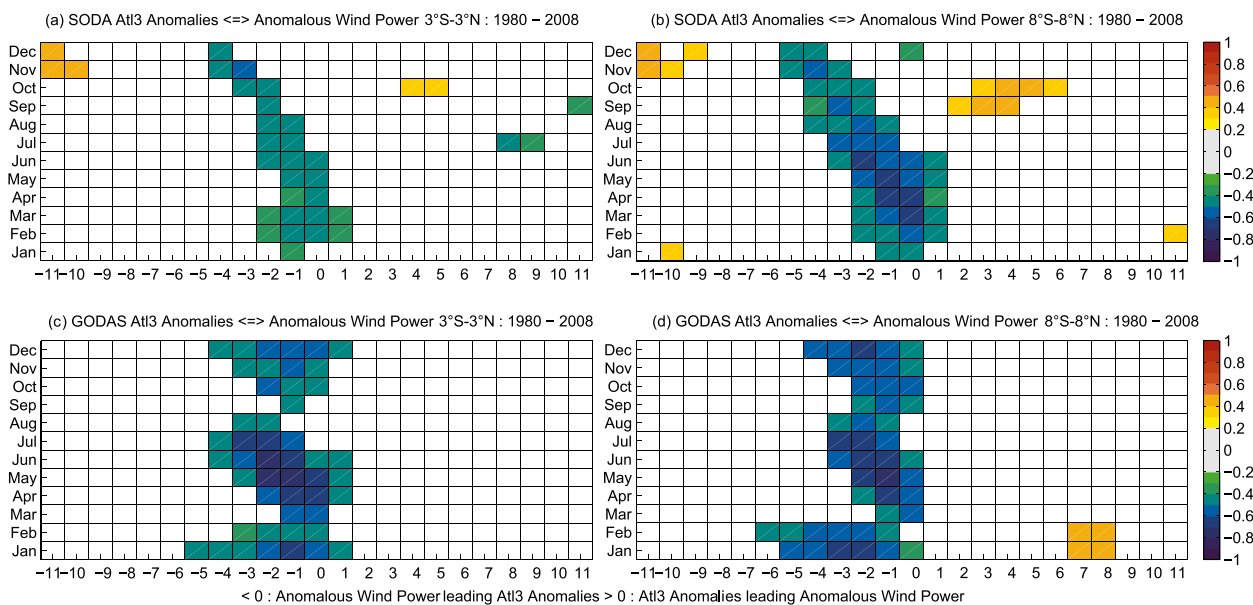


FIG. 2. Monthly stratified cross correlation between full wind power anomalies averaged over (a),(c) 3°S–3°N and (b),(d) 8°S–8°N and AtI3 SST anomalies from (a),(b) SODA (1980–2008) and (c),(d) GODAS (1980–2008). A 3-month running mean has been applied to the data prior to doing the correlation analysis. Only values significant at the 95% level according to a Student's *t* test are shown.

interannually, especially between the months of April and August and between November and January (Burls et al. 2012). Studies of tropical Atlantic upper-ocean energetics (Burls et al. 2011, 2012) have shown that changes in the available potential energy of the tropical Atlantic are primarily driven by zonal wind power fluctuations. Forcing available potential energy (APE) changes, fluctuations in tropical Atlantic zonal wind power are therefore seen to lead SST anomalies in the eastern Atlantic by 1–4 months. Extending the domain over which APE is evaluated from the equatorial region (3°S–3°N) to include the tropical domain (8°S–8°N) reduces the most important processes governing APE variability down to one dominant process: namely, seasonal fluctuations in the work done by the wind over the tropical Atlantic domain (Burls et al. 2011, see their Figs. 4 and 5). For the equatorial domain, changes in APE are controlled not only by wind power fluctuations but also by anomalous processes acting at the boundaries as transients enter and exit the domain. As a result, wind power acting between 8°N and 8°S is a better predictor for anomalous AtI3 SST than wind power between 3°N and 3°S (Fig. 2). The meridional extent of the tropical domain chosen as 8°S–8°N is deemed large enough to encompass the wind forced region over which seasonal buoyancy power changes are predominantly related to wind power fluctuations yet small enough to preserve the strong relationship between AtI3 SST and APE as well as limit the lag-lead in this relationship (Burls et al. 2011, 2012).

The wind power term within the kinetic energy evolution equation is defined as

$$\Phi_{\text{ww}} = \iint_{z=0} \mathbf{v} \cdot \boldsymbol{\tau}_s dS = \iint_{z=0} (u\tau_s^x + v\tau_s^y) dS, \quad (1)$$

where the double integral is a surface integral evaluated at the surface of the ocean, $z = 0$, $\mathbf{v} = (u, v)$ is the horizontal velocity field, and $\boldsymbol{\tau}_s$ is the surface wind stress. The zonal component of the wind power term ($\Phi_{\text{ww}^x} = \iint_{z=0} u\tau_s^x dS$) integrated over the tropical Atlantic (8°S–8°N, 60°W–15°E) is the dominant source of fluctuations in the buoyancy power term within the kinetic energy evolution equation. The buoyancy power term is a reversible exchange term within the available potential energy evolution equation and, when integrating over the tropical Atlantic, is the dominant term driving available potential energy changes (Burls et al. 2011, 2012). In this study, we use monthly wind stress and surface velocity fields to estimate tropical Atlantic wind power, making the assumption that $\overline{u\tau_s^x} \approx \overline{u}\overline{\tau_s^x}$. We have attempted to estimate the size of the eddy term by comparing estimates of the time-mean tropical Atlantic wind power based on 2-day averages of surface wind stress and currents against estimates based on monthly-mean values from a Regional Ocean Modeling System (ROMS) tropical Atlantic (TAtI) simulation [as presented in Burls et al. (2011, 2012)]. The contribution of the eddy term is approximately 12% of the total. More generally, according to observationally based

time-mean estimates of wind power integrated over the latitude band between 3°S and 3°N presented in Scott and Xu (2009, their Table 1), the contribution of the eddy term is approximately 23% of the total.

When trying to identify the source of wind power anomalies with respect to the seasonal cycle, it is insightful to decompose the tropical Atlantic zonal wind power term,

$$\begin{aligned}\Phi_{\text{ww}^x} &= \iint_{z=0} u \tau_s^x dS \\ &= \iint_{z=0} (\bar{u} + u')(\bar{\tau}_s^x + \tau_s^{x'}) dS \\ &= \underbrace{\iint_{z=0} \bar{u} \bar{\tau}_s^x dS}_{\Phi_{\text{ww}^x}^{\text{cl}}} + \underbrace{\iint_{z=0} \bar{u} \tau_s^{x'} dS}_{\Phi_{\text{ww}}^{\text{mupr}}} + \underbrace{\iint_{z=0} u' \bar{\tau}_s^x dS}_{\Phi_{\text{ww}}^{\text{m7pu}}} + \underbrace{\iint_{z=0} u' \tau_s^{x'} dS}_{\Phi_{\text{ww}}^{\text{pp}}},\end{aligned}\quad (2)$$

where $\Phi_{\text{ww}^x}^{\text{cl}}$ is the climatological component, $\Phi_{\text{ww}}^{\text{mp}} = \Phi_{\text{ww}}^{\text{mupr}} + \Phi_{\text{ww}}^{\text{m7pu}}$ is the mean-perturbation component, and $\Phi_{\text{ww}}^{\text{pp}}$ is the perturbation component. The terms $\bar{\tau}_s^x$ and \bar{u} represent the climatological zonal wind stress and surface current values, while $\tau_s^{x'}$ and u' represent interannual perturbations from these climatological fields. The mean-perturbation component $\Phi_{\text{ww}}^{\text{mp}}$ comprises two terms, $\Phi_{\text{ww}}^{\text{mupr}} = \iint_{z=0} \bar{u} \tau_s^{x'} dS$, which represents the effects of anomalous zonal wind stress fluctuations acting on climatological surface currents, and $\Phi_{\text{ww}}^{\text{m7pu}} = \iint_{z=0} u' \bar{\tau}_s^x dS$, representing the effects of climatological winds acting on anomalous surface current variations.

Following Eq. (2), anomalous wind power approximated by its zonal component consists of three components,

$$\Phi_{\text{ww}^x}^{\text{ano}} = \Phi_{\text{ww}}^{\text{mupr}} + \Phi_{\text{ww}}^{\text{m7pu}} + \Phi_{\text{ww}}^{\text{pp}}. \quad (3)$$

Anomalous tropical Atlantic wind power is determined primarily by the mean-perturbation terms $\Phi_{\text{ww}}^{\text{mupr}}$ and $\Phi_{\text{ww}}^{\text{m7pu}}$, with fluctuations in the perturbation term $\Phi_{\text{ww}}^{\text{pp}}$ playing a much smaller secondary role (Burls et al. 2012). The term $\Phi_{\text{ww}}^{\text{mupr}}$ captures the role of the atmosphere through either remotely forced wind stress fluctuations, stochastic wind forcing, or local wind stress fluctuations associated with an anomalous seasonally excited Bjerknes feedback. The term $\Phi_{\text{ww}}^{\text{m7pu}}$ captures the role of oceanic adjustment. From an energetics perspective, $\Phi_{\text{ww}}^{\text{m7pu}}$ shows the effects of the delayed, negative, ocean memory feedback mechanism. In the Pacific, this term is seen to be responsible for the transition from El Niño to La Niña (Goddard and Philander 2000). Similarly, surface current changes associated with transients affect the ability of the wind to do work on the ocean in the Atlantic and contribute to the decay of anomalous AtI3 SST events (Burls et al. 2012).

While both of these mean-perturbation terms contribute to anomalous tropical Atlantic wind power, the focus

of this paper is on the role of remote atmospheric forcing, so we concentrate purely on the role of $\Phi_{\text{ww}}^{\text{mupr}}$, isolating the role of anomalous atmospheric conditions from anomalous oceanic conditions. Essentially this amounts to a physically motivated way of assessing the importance of interannual wind stress perturbations. Interannual wind stress anomalies in regions where climatological currents are strong have a far greater impact on AtI3 SST. Therefore, for the remainder of this paper, when we refer to anomalous wind power, we are in fact only referring to the $\Phi_{\text{ww}}^{\text{mupr}}$ component of $\Phi_{\text{ww}^x}^{\text{ano}}$. It is worth noting that the assimilation of data within the GODAS and SODA reanalysis implies that energy is not strictly conserved by the ocean model. While a fully closed energy budget is unlikely, we make the assumption that the reanalysis is doing a relatively good job of capturing the wind stress and surface current fluctuations associated with the assimilated AtI3 SST fluctuations.

As wind power is a noisy signal relative to tropical Atlantic APE and AtI3 SST anomalies, which, forced by the wind power anomalies, are the integral of wind power anomalies over the previous months, a 3-month running mean has been applied prior to the correlation analysis including wind power (Figs. 2, 3, 5, and 6). While significant correlations are seen without applying a running mean, it acts to capture the integrated effect of wind power forcing over the previous months.

3. Results

a. Connection between tropical wind power and SST anomalies in the eastern equatorial Atlantic

Monthly correlations between both anomalous western equatorial Atlantic (WEA) wind stress and tropical wind power (approximated by $\Phi_{\text{ww}}^{\text{mupr}}$) on the one hand and AtI3 SST anomalies on the other hand from both SODA and GODAS show that anomalously weak (strong) wind power and wind stress in the first

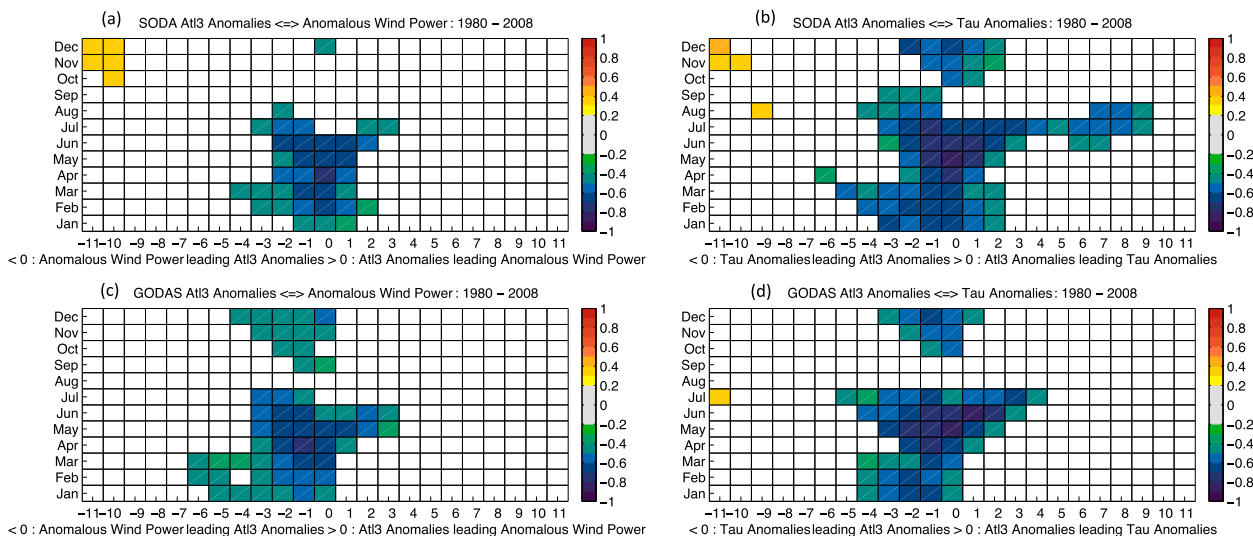


FIG. 3. Monthly stratified cross correlation between (a),(c) tropical wind power and (b),(d) western equatorial Atlantic wind stress anomalies (40° – 10° W, 2° S– 2° N) and AtI3 SST anomalies from (a),(b) SODA (1980–2008) and (c),(d) GODAS (1980–2008). A 3-month running mean has been applied to the data prior to doing the correlation analysis. Only values significant at the 95% level according to a Student's t test are shown.

half of the calendar year are associated with warm (cold) EEA surface waters in the following months (Fig. 3). Correlations for wind stress are particularly high during the months of May–July when the seasonally excited Bjerknes feedback plays a role in the development of the cold tongue.

The monthly lag–lead correlations are roughly symmetric about zero lag between April and June. This symmetric lag–lead relationship suggests that EEA SST and tropical wind power anomalies reinforce one another as opposed to purely a one-way forcing of EEA SST anomalies by tropical wind power anomalies. Symmetric lag–lead correlations suggest that the covariability observed is the result of a positive feedback with anomalies in each variable reinforcing one another (Frankignoul and Hasselmann 1977). This finding is consistent with our understanding that EEA SST anomalies grow through the Bjerknes feedback during these months (Keenlyside and Latif 2007).

Figure 3 indicates that AtI3 SST anomalies and tropical wind power as well as wind stress anomalies reinforce one another between April and July as an anomalous evolution of the Bjerknes feedback that is seasonally excited during these months: also referred to as the seasonally excited thermocline mode (Ding et al. 2009; Burls et al. 2011). But what factors result in the anomalous evolution of this seasonally excited Bjerknes feedback? In the following section we address the following question: what is the role of the SAA in exciting wind stress and wind power anomalies and hence interannual SST variability in the EEA?

b. Connection between the SAA and tropical wind power

The correlation between time series of tropical wind power anomalies and fields of sea level pressure anomalies for all calendar months at zero lag shows a pattern reminiscent of the SAA. Looking at lead–lag correlation pattern for the individual calendar months there are a few combinations that stick out: The highest maximum correlation is found for February wind power anomalies and February SLP anomalies with values above 0.6 between both SODA wind power anomalies and ERA-Interim SLP and GODAS wind power anomalies and NCEP-2 SLP. Values are higher for the latter (Fig. 4). Very similar patterns are found for correlations between SODA wind power and NCEP-2 SLP and GODAS wind power and ERA-Interim SLP, respectively, with the position of the maximum correlation determined by the reanalysis product used to calculate the wind power time series (not shown). The second highest correlations occur for October wind power anomalies and October SLP. In GODAS, high SAA-like correlation patterns are also found for March, April, and September. Thus, there are two seasonal bands of connection between the South Atlantic anticyclone and the equatorial wind power anomalies, one in February–April and the other in September–October. These results suggest that variability in the strength of the SAA influences wind power over the tropical Atlantic, mainly in the months leading up to the seasonal development of the cold tongue in May–June and the secondary cooling event in November–December that is

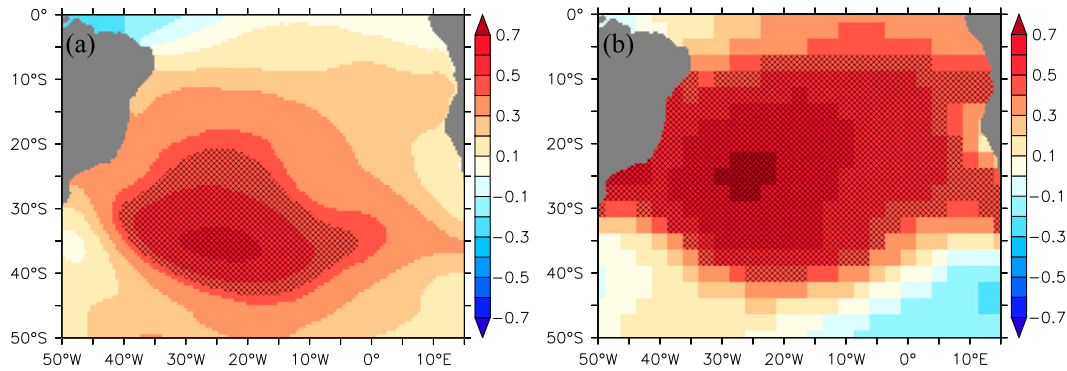


FIG. 4. Correlation between February tropical wind power anomalies and February SLP from (a) SODA and ERA-Interim (1980–2008) and (b) GODAS and NCEP-2 (1980–2008). Hatching indicates values significant at the 95% level.

also associated with interannual Atlantic Niño-like events (Okumura and Xie 2006).

The connection between fluctuations in the SAA and changes in tropical wind power is likely due to both the direct influence on the southeasterly trades—as the strength of the trade winds is dependent on the pressure difference between tropics and subtropics—and thermal air–sea interaction that gradually moves SLP anomalies toward the equator. Huang and Shukla (2005) describe how atmospheric disturbances associated with the SAA induce anomalous winds and surface heat fluxes at its northern flank, thereby generating SST anomalies that in turn impact local SLP, which leads to a northward shift of the disturbances.

To better illustrate the correlations between individual calendar months, a SAA index is calculated by averaging interannual SLP anomalies over 40°–10°S, 40°–10°W; this index is correlated with the tropical wind power anomalies for every calendar month combination (Figs. 5a,c). The results from SODA and GODAS agree well with respect to the two seasonal maxima around February and October. February and March SAA anomalies appear to be most influential with high correlations, both instantaneous and in the following months up to July. As seen in Fig. 3, western equatorial wind stress alone is significantly correlated with Atl3 SST anomalies. Figures 5b,d thus assess the relationship between the SAA index and western equatorial wind stress. While the pattern

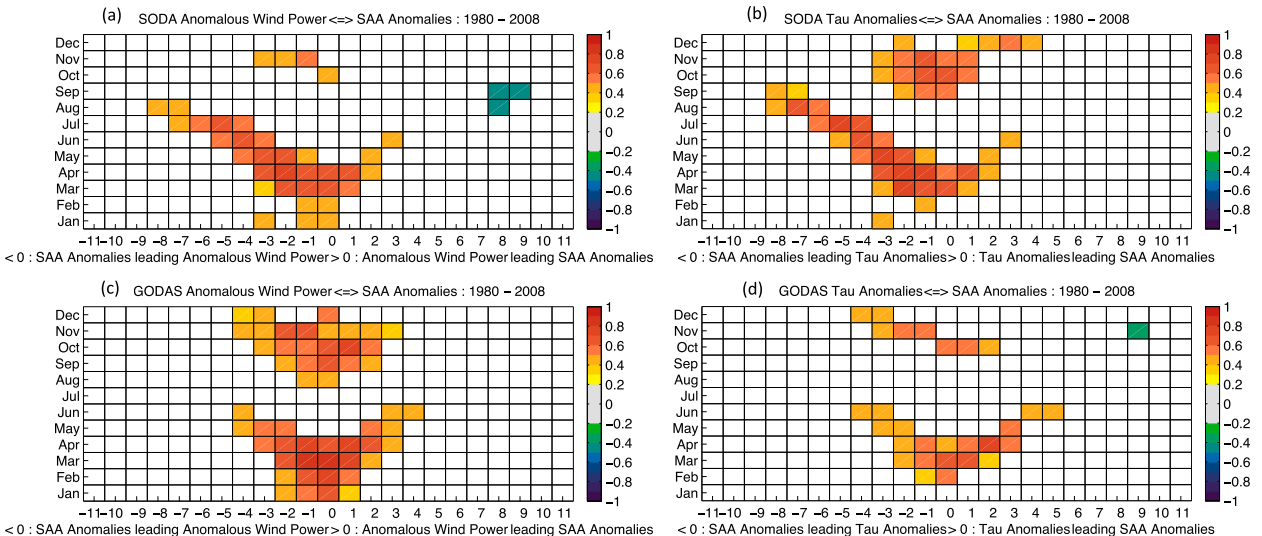


FIG. 5. Monthly stratified cross correlation between the SAA index and (a),(c) tropical wind power anomalies and (b),(d) western equatorial wind stress anomalies, from (a),(b) SODA and ERA-Interim and (c),(d) GODAS and NCEP-2. All time series are for 1980–2008. A 3-month running mean has been applied to the data prior to doing the correlation analysis. Only values significant at the 95% level according to a Student’s *t* test are shown.

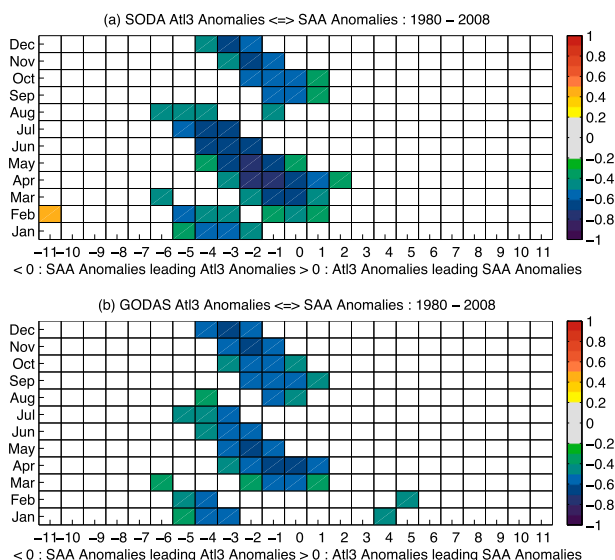


FIG. 6. Monthly stratified cross correlation between the SAA index and Atl3 SST anomalies from (a) SODA and ERA-Interim (1980–2008) and (b) GODAS and NCEP-2 (1980–2008). A 3-month running mean has been applied to the data prior to doing the correlation analysis. Only values significant at the 95% level according to a Student's t test are shown.

is very similar to the correlation between the SAA variability and anomalous wind power, using wind power results in stronger correlations at zero lag in February and March: that is, in the months that appear to play the key role in affecting the seasonally excited Bjerknes feedback. This difference between western equatorial wind stress and tropical wind power is due to the fact that wind power takes into account 1) the full region over which wind stress variability affects equatorial SSTs and 2) the state of the ocean that the wind stress anomaly is acting on. Ultimately, it is wind power, not wind stress, that drives changes in the available potential energy (thermocline slope) of the equatorial ocean. Note that, since climatological westward surface currents (i.e., currents in the same direction as the trade winds) are stronger south of the equator, zonal wind stress anomalies will translate into stronger wind power anomalies when they occur south of the equator.

While Fig. 3 shows the seasonal dependence in wind power–Atl3 SST lag–lead correlations and Fig. 5 shows the equivalent for wind power–SAA index correlations, Fig. 6 shows the resulting seasonal dependence in the correlation between the SAA index and Atl3 SST anomalies. Given that wind power anomalies are seen to lead JJA Atl3 anomalies by 1–3 months (Fig. 3) and that these March–June wind power anomalies are in turn led by SAA anomalies by between 1 and 4 months (Fig. 5), in Fig. 6 we see significant correlations between JJA Atl3 SST anomalies and February–April SAA anomalies.

In summary, tropical wind power anomalies are significantly influenced by the variations in the South Atlantic anticyclone. The connection is strongest in February and March, presumably because there are no strong local dynamical feedbacks acting within the equatorial Atlantic at this time of year so that the equatorial Atlantic is then more sensitive to remotely forced perturbations in the southeasterly trades. These results suggest that a stronger than normal SAA kicks off an intensification of the trade winds and thus results in an early onset of the seasonally excited Bjerknes feedback. Conversely, a weaker than normal SAA resulting in weaker than normal trades could result in a delay in the onset of the seasonally excited Bjerknes feedback. Consistent with this interpretation, we find significant correlations between variability in the SAA in March and western equatorial Atlantic wind stress in the following months as well as between WEA wind stress and Atl3 SST between May and July. Analyzing tropical wind power in addition to WEA wind stress gives a stronger relationship with the SAA and results in an extra month of lead time. In addition to the shift in trade wind onset, anomalously strong or weak wind power might impact the intensity of the cold tongue development.

c. Individual strong connection years

To investigate the link between the SAA, winds, and ultimately cold tongue SST in more detail, Figs. 7 and 8 show a composite of individual warm and cold event years with a strong connection among SAA, wind power, and SST. Strong connection years for the time period 1980–2008 are identified based on the ERA-Interim SAA index from February to May, SODA anomalous tropical wind power (Φ_{ww}^{mupr}) from February to June, and SODA June–August Atl3 SST anomalies—selecting years in which the monthly anomaly exceeds 70% of the standard deviation of the detrended time series in at least two of those months for all three variables. Based on this threshold we find that the cold event years of 1982, 1983, 1992, and 1997 as well as the warm event years of 1984, 1988, 1995, and 2008 are strong connection years. Thus the strong connection years represent about half of all Atlantic warm and cold event years occurring between 1980 and 2008. The observed cold event of 2004 is not well represented in SODA and thus does not qualify as a strong connection year although it was preceded by a strong wind power anomaly. Using GODAS and NCEP-2 or including more years in the assessment of the relationship between SAA and wind power by removing the SST component from the selection criteria gives very similar results to the ones shown in Fig. 7.

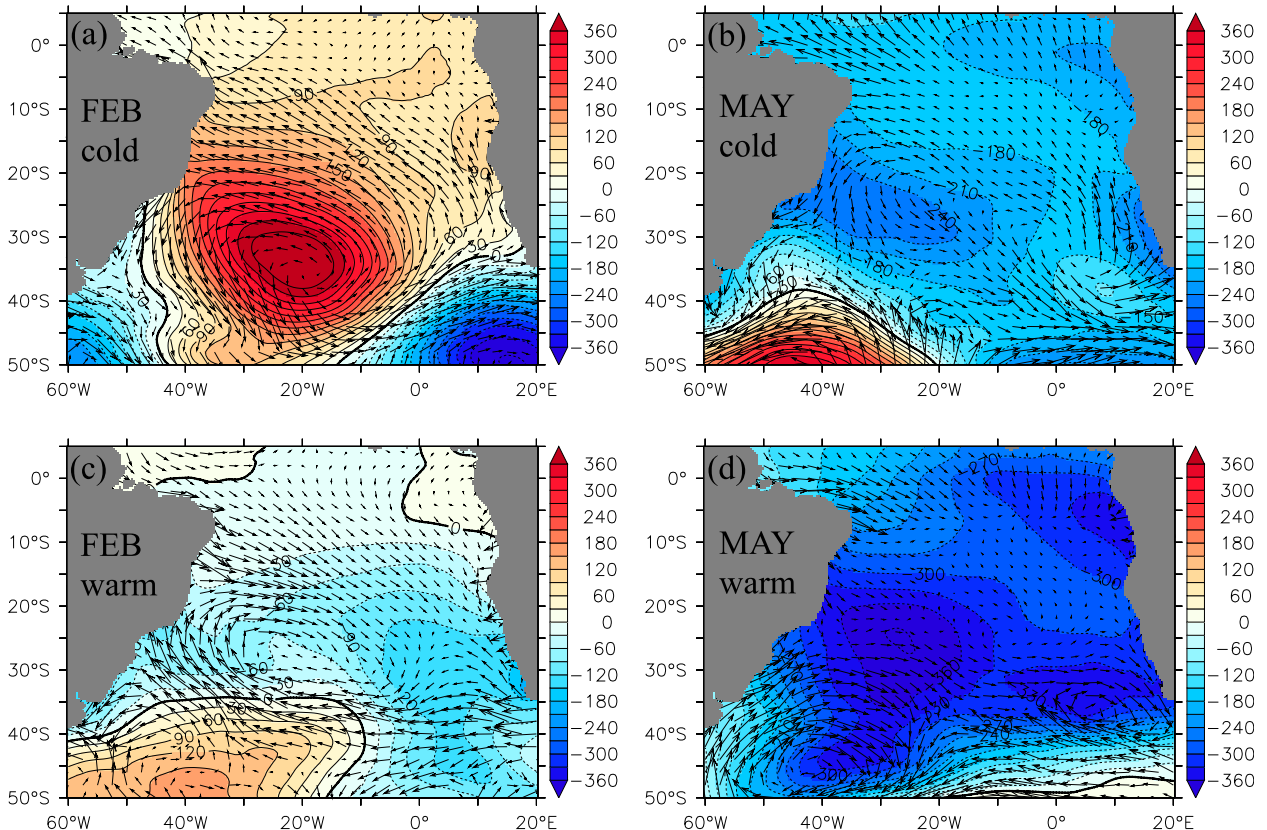


FIG. 7. SLP (hPa) and wind stress anomaly composite from ERA-Interim for (a) February and (b) May of cold strong connection years and (c) February and (d) May of warm strong connection years.

In the strong connection years, the strength of the SAA between February and May is associated with wind power anomalies over the following months and a shift in timing of the cold tongue onset in the eastern equatorial Atlantic, producing SST anomalies there (Figs. 7, 8). We find that, in years in which the influence of the SAA on wind power persists over several months, the cold tongue SST is more likely to be impacted. We suspect that these are years in which local forcing is less important so that an early onset of the trades actually translates to a shift in the timing of the cold tongue onset.

It is interesting to note that the timing of the SAA impact is not completely symmetric for cold and warm event years. In the cold years, the strongest SAA anomaly is clearly found in February (Fig. 7a) and March while the situation has already reversed with weaker than normal SLP in May (Fig. 7b). The SLP composite for the warm years on the other hand only shows a slight weakening for February (Fig. 7c) that persists and gets stronger in May (Fig. 7d). A strengthening of the SAA in February and March (Fig. 7a) is associated with positive tropical wind power and WEA wind stress anomalies from February to June (Fig. 8a) that results in an early onset

and amplification of the cold tongue (Fig. 8b) and subsequent cold SST anomalies in JJA (Fig. 8d). An anomalously weak SAA (Figs. 7c,d) is associated with negative tropical wind power and WEA wind stress anomalies from March to June (Fig. 8a), leading to a late cold tongue onset as well as a suppression in cold tongue development (Fig. 8b) and thereby warm SST anomalies in JJA (Fig. 8c). The wind stress anomaly associated with the SAA anomaly is found to be strongest south of the equator (Figs. 7a,c,d). Only in May of the cold years, the strongest wind stress anomaly is almost centered on the equator. By that time, the Bjerknes feedback on the equator has kicked in, leading to stronger trade winds on the equator despite the weaker SAA (Fig. 7b).

4. Discussion

a. Possible mechanisms

We have shown that variations in the strength of the SAA can influence interannual variability in JJA SST in the eastern equatorial Atlantic by affecting both timing of the onset and strength of the cold tongue. For all years

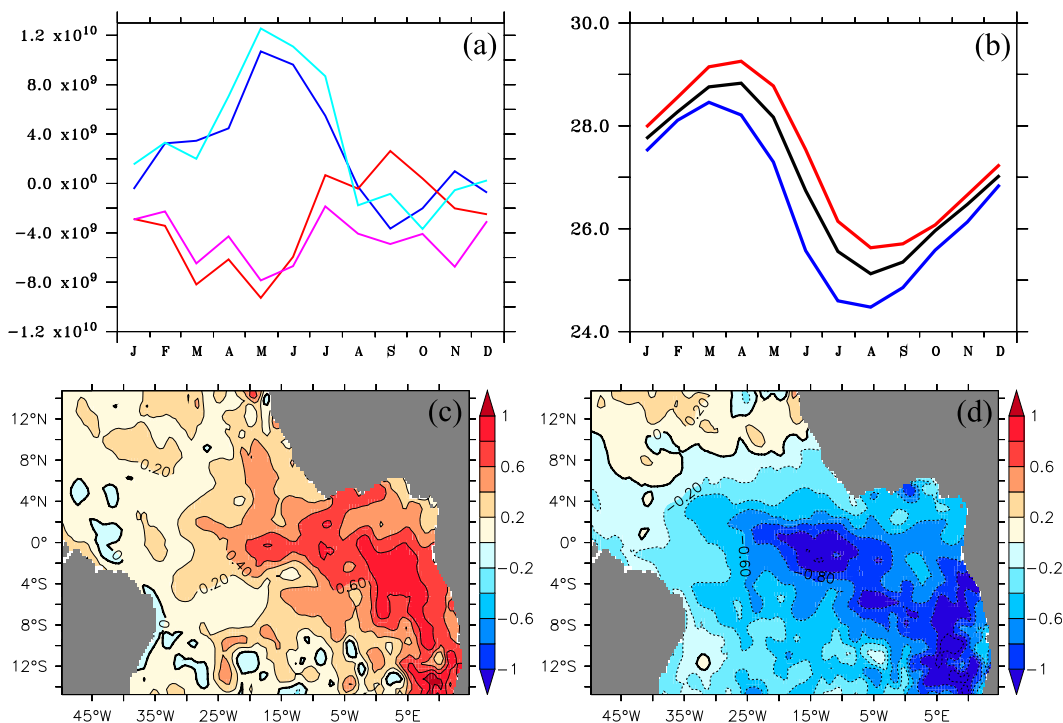


FIG. 8. Composite of strong SAA connection years for cold and warm events: (a) anomalous wind power (J s^{-1}) in cold (blue) and warm (red) strong connection years from SODA as well as WEA wind stress ($10^{-12} \text{ N m}^{-2}$) in cold (light blue) and warm (magenta) strong connection years; (b) At13 SST ($^{\circ}\text{C}$) in cold (blue) and warm (red) strong connection years and climatological seasonal cycle (black) from SODA; (c) SST anomaly ($^{\circ}\text{C}$) for JJA in warm strong connection years from SODA; and (d) SST anomaly ($^{\circ}\text{C}$) for JJA in cold strong connection years from SODA.

that we identified as strong connection years, we see a SAA anomaly giving rise to a zonal wind stress anomaly with a maximum south of the equator (Figs. 7a,c,d). Looking at the whole tropical region (8°S – 8°N , 60°W – 15°E), this causes a wind power anomaly (Fig. 8a), resulting in an APE anomaly and a SST anomaly in the south eastern part of the basin (Figs. 8c,d). From a more local perspective, the wind stress curl anomaly that results from the SAA wind stress anomalies causes an upper-ocean temperature anomaly south of the equator (Fig. 9). This upper-ocean temperature anomaly south of the equator translates into an equatorial anomaly via one or a combination of several mechanisms that are discussed below. Once the SST anomaly has started to develop in the At13 region, it can be reinforced between April and August by the anomalous evolution of the Bjerknes feedback that is seasonally excited during these months (Ding et al. 2009; Burls et al. 2011).

There are several possible mechanisms by which SAA-induced variations in tropical wind power actually affects SST in the EEA. The simplest way to impact SST in the eastern equatorial Atlantic are zonal wind stress changes in the western equatorial Atlantic that excite

Kelvin waves propagating to the east. Although the strongest wind stress anomalies associated with the SAA occur south of the equator (Fig. 7), corresponding anomalies can be found in the western equatorial region (Fig. 8a). Maps of zonal wind stress anomalies for all calendar months of the individual strong connection years indicate, however, that the anomalies occur first south of the equator in February–March while wind stress anomalies on the equator are established between April and June in most years (not shown). This suggests that the wind stress anomalies in the WEA might be partly associated with a Bjerknes response to anomalies in the east. We conclude that, while western equatorial zonal wind stress anomalies associated with the SAA variations are playing a role in the development of warm and cold anomalies in the eastern part of the basin, there are additional mechanisms at work that communicate the effects of wind anomalies south of the equator to the EEA.

One possibility is an ocean adjustment to the wind anomaly via the propagation of Rossby and Kelvin waves. This mechanism has been shown to be at work from the northern tropical Atlantic by Foltz and McPhaden (2010)

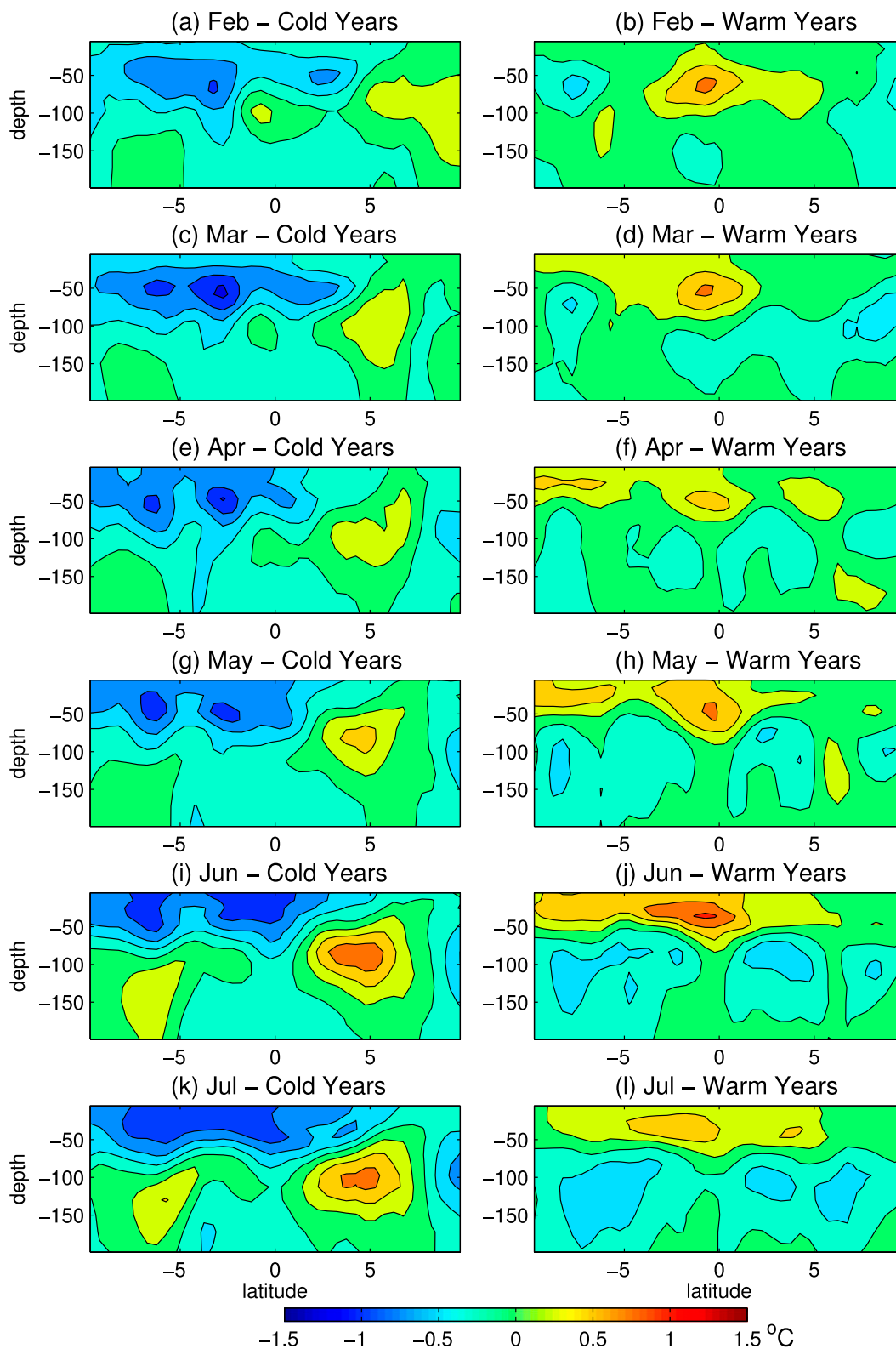


FIG. 9. SODA composites of zonal-mean upper-ocean temperature anomalies averaged across the entire Atlantic basin for warm and cold strong connection years.

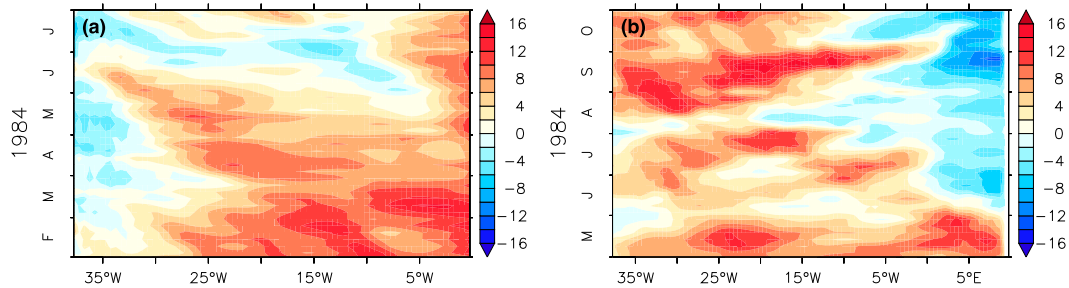


FIG. 10. Longitude vs time diagrams (5-day average data) of the depth of the 23°C isotherm anomalies (m) from a Nucleus for European Modelling of the Ocean (NEMO) ORCA05 ocean model simulation (a) averaged over 2°–5°S for February–July 1984 and (b) averaged over 2°S–2°N for May–October 1984; positive values denote a deepening of the thermocline. The model simulation has been compared to observations and used to illustrate Rossby and Kelvin wave propagation in the northern tropical Atlantic in Lübbcke and McPhaden (2012).

and Lübbcke and McPhaden (2012) in response to wind variations associated with the meridional mode and Pacific El Niño events, respectively. We find indications for this mechanism being active in some of the years. For example, in 1984, there is a wind stress curl anomaly at about 5°S, 15°W, followed by a westward-propagating thermocline depth anomaly along 2°–5°S, indicative of a Rossby wave, that is reflected into an eastward-propagating equatorial thermocline anomaly, indicative of an equatorial Kelvin wave (Fig. 10). In other strong connection years, however, there is no clear indication of wave propagation.

A second possibility is the meridional advection of subsurface temperature anomalies toward the equator that has been discussed by Richter et al. (2013) for the northern tropical Atlantic. Also, Perez et al. (2013) suggested from observationally based estimates of meridional currents in the eastern equatorial Atlantic that interannual variations in the subsurface branches of the tropical cells can result in equatorward advection of temperature anomalies induced near the equator. Subsurface temperature anomalies consistent with the anomalous wind stress curl are indeed found south of the equator between 30°W and 0° for all strong connection years, and there is a consistent connection between these upper-ocean temperature anomalies south of the equator and on the equator (Fig. 9). It is, however, hard to find evidence for the actual advection of the subsurface temperature anomalies toward the equator. Surface layer heat budget analyses for the individual strong connection years suggest that meridional advection is important in some of the years but not in others (Fig. 11). Vertical temperature advection dominates each event, consistent with our understanding that an anomalous seasonally excited Bjerknes feedback plays a central role in the development of JJA SST anomalies within the Atl3 region. However, for April–May of cold event years 1982 and 1997, anomalous meridional

temperature advection appears to be playing a key role in bringing on the cooling in later months (Figs. 11a,b). The same is true for March of the 1988 and 1995 warm event years (Figs. 11c,d).

The third mechanism we explored is the role of intraseasonal wind variations that impact SST via mixing. Marin et al. (2009) showed that the early cold tongue onset in 2005, although preconditioned by a remotely forced shoaling of the thermocline, was triggered by a sudden intensification of local mixing in response to strong southerly winds. Brandt et al. (2011) concluded that local intraseasonal wind fluctuations that are connected to the SAA contribute to variability in the onset and strength of the Atlantic cold tongue. The daily wind stress magnitudes from ERA-Interim averaged over 10°W–0° for April–August of the years identified as warm and cold strong connection years suggest that the strong intraseasonal wind stress intensification south of the equator in May of 1997 played a key role in the cooling of that year and that the wind stress intensification toward the end of May/beginning of June in 1992 contributed to that year's cold event [Fig. 12; analogous to Fig. 7 from Marin et al. (2009) for 2005 and 2006]. Consistent with expectations for warm event years, the seasonal wind stress intensification is substantially weaker in 1984 and 1988. However, there is a pronounced wind stress intensification in May of the warm event year of 1995 and no such intensification in the cold event year 1983. Thus, intraseasonal wind stress variations south of the equator appear to play a role in some of the events but do not provide a consistent explanation for all strong connection years.

We conclude that the relation between the SAA-induced wind stress variations south of the equator and eastern equatorial SST cannot be attributed to one single mechanism. Zonal wind stress changes in the western equatorial basin, wave adjustment, meridional advection of subsurface temperature anomalies, intraseasonal

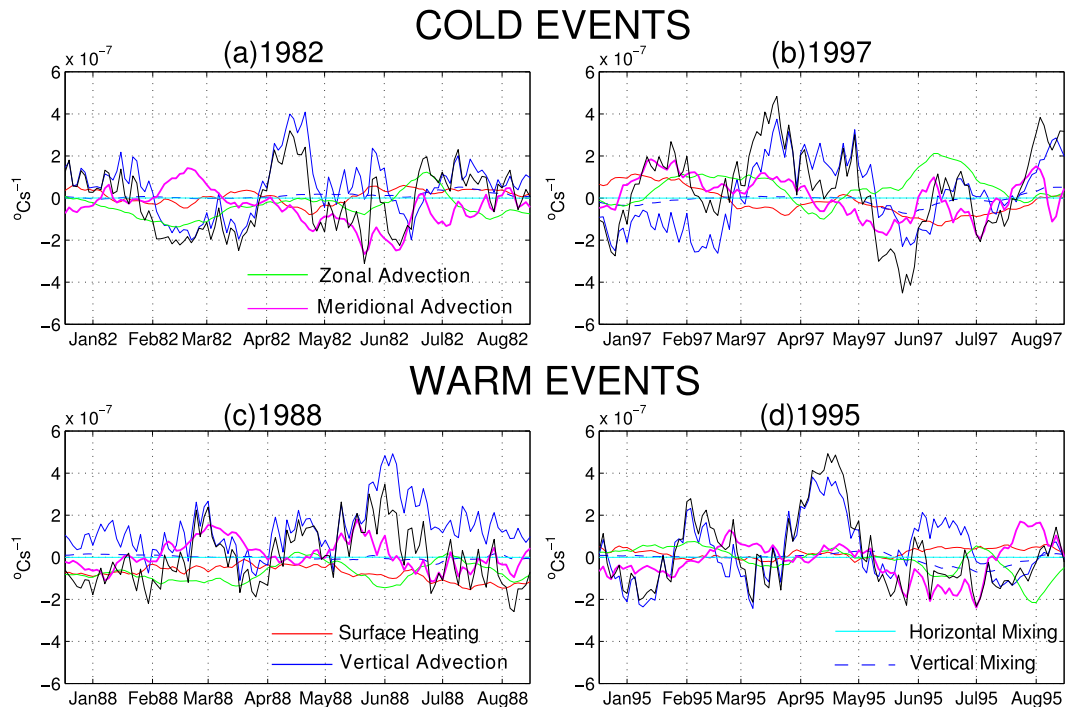


FIG. 11. Anomalies in the heat budget terms contributing to interannual variations in the average temperature of the warm water layer (WWL) over the Atl3 region (using a fixed depth of 70 m, which corresponds to the mean depth of the thermocline). This heat budget analysis is based on a simulation of oceanic conditions within the tropical Atlantic between 1980 and 2004 conducted using ROMS. Referred to as ROMS-TAtl, this simulation is validated and analyzed in Burls et al. (2011, 2012) [see Fig. 11 in Burls et al. (2011) and Fig. 1 in Burls et al. (2012)]. A 14-day running mean has been applied to the time series to smooth out the high-frequency variability.

wind stress variations, and possibly even other mechanisms all play a role to varying degrees in different years.

b. Influence of ENSO on SAA variability

The importance of variations in the strength of the SAA in forcing Atlantic Niño and Niña events leads to the question of what drives the SAA variability. The variability of sea level pressure in the South Atlantic has been found to be largely independent of that in other ocean basins. Richter et al. (2014) suggest that modulations in the SAA might be linked to a shift in the Atlantic ITCZ. Sterl and Hazeleger (2003) show that the correlation between SLP anomalies in the SAA region and elsewhere is small everywhere outside the South Atlantic and conclude that the SAA variability is not related to the North Atlantic Oscillation (NAO) and only weakly related to the Pacific ENSO. Colberg et al. (2004), on the other hand, suggest that ENSO does have an influence on the South Atlantic. Also, Mo and Häkkinen (2001) and Huang (2004) describe an El Niño influence on the South Atlantic via the Pacific–South American (PSA) pattern. Composites of December–February (DJF) tropical Pacific SST anomalies for the strong connection years defined in section 3c show that

warm strong connection years tend to be associated with Pacific La Niña conditions while cold strong connection years tend to occur during Pacific El Niño conditions (Fig. 13). The relation is, however, not completely consistent for DJF before the strong connection year events in summer. Two of the warm events were preceded by La Niña and two were preceded by El Niño, while two of the cold events were preceded by El Niño and two were preceded by neutral conditions in the tropical Pacific. There is no significant correlation between Niño-3 (5°S–5°N, 150°W–90°E) SST anomalies and the SAA index for both Niño-3 SSTAs leading and lagging the SAA index by 0–12 months. Composites of Southern Hemisphere 500-hPa geopotential height anomalies for the strong connection years also do not indicate an obvious relation to ENSO forcing (not shown). While these results do not suggest a major role for ENSO influence on variations of the South Atlantic anticyclone, at least not in years in which variations in the SAA translates into EEA SST anomalies, the connection might be stronger during other El Niño years and for other seasons. Mo and Häkkinen note that the relationship between ENSO and SSTAs in the South Atlantic is highly seasonally dependent and strongest in September–November. As

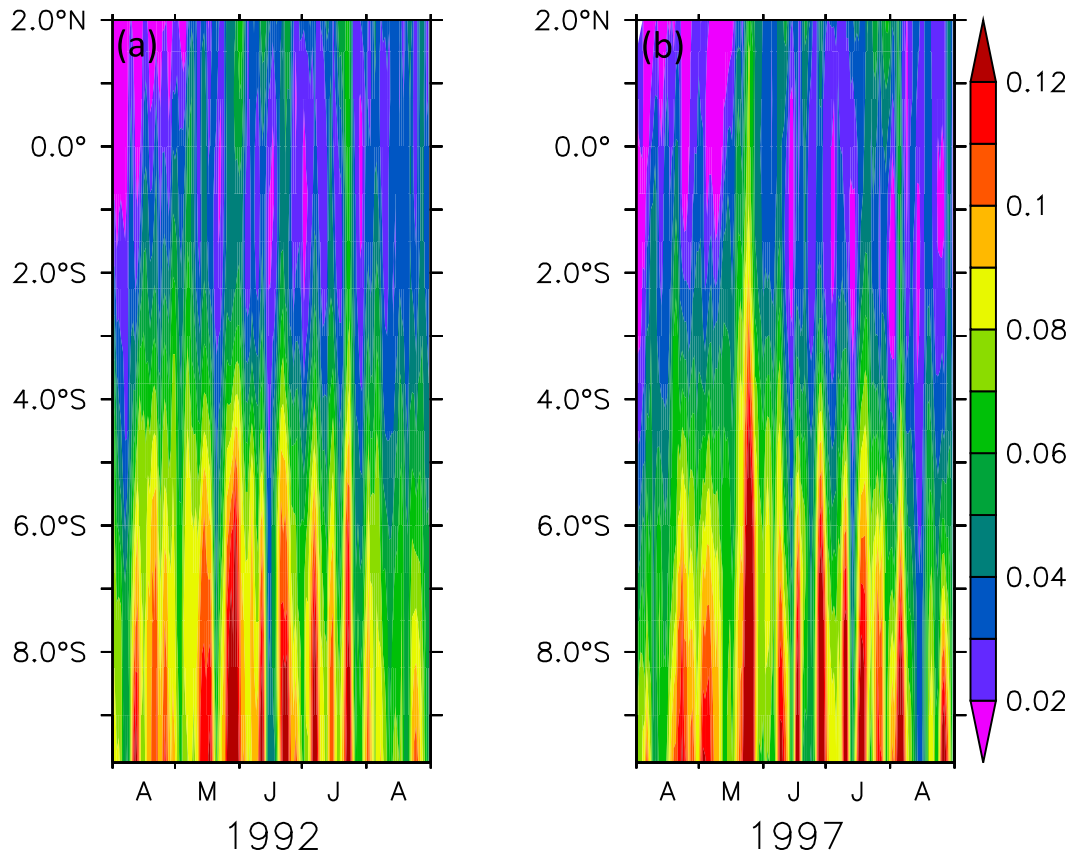


FIG. 12. Daily wind stress magnitude from ERA-Interim averaged over 10°W – 0° for April–August of the strong cold connection years 1992 and 1997.

our analysis is focusing on years with anomalous conditions in the South Atlantic in February–July, we might not capture these signals.

Tropical Pacific SST anomalies are stronger and more consistent in the years following the SST anomalies in the tropical Atlantic (Figs. 13b,d). All Atlantic strong connection warm events were followed by Pacific La Niñas and two of the cold events were followed by El Niño events. This is in agreement with studies by Rodríguez-Fonseca et al. (2009) and Ding et al. (2011) showing that SST anomalies in the equatorial Atlantic may impact the development of Pacific El Niño and La Niña events through changes in the Walker circulation. The question, however, of what ultimately drives SAA variability is beyond the scope of this study.

5. Summary

In this study, the connection between variations in the strength of the South Atlantic subtropical high pressure system and SST anomalies in the eastern equatorial Atlantic has been investigated using ocean and atmospheric reanalysis data. We find that, for years

with an anomalously strong SAA in February and March, the SAA anomaly results in the early onset and amplification of the cold tongue, while, for years with an anomalously weak SAA that persists until May, it results in the suppression of cold tongue development as well as delayed onset on some occasions. The SAA thus appears to influence both timing and intensity of the cold tongue development, but the modulation of the timing is more important for cold events. An early cold tongue onset and an amplification of its intensity is associated with cold JJA SST anomalies or Atlantic Niña events, while a late onset and suppression of the cold tongue development result in warm anomalies or Atlantic Niño events. The communication between SAA strength and SST happens via work done by the wind on the tropical Atlantic Ocean: namely, the wind power. We find anomalous high wind power in February–June in response to a strengthening of the SAA. Consistent with the results by Burls et al. (2012), high wind power in the first half of the year is associated with cold anomalies in JJA. Analogously, anomalously low wind power following a weakening of the SAA then results in warm anomalies.

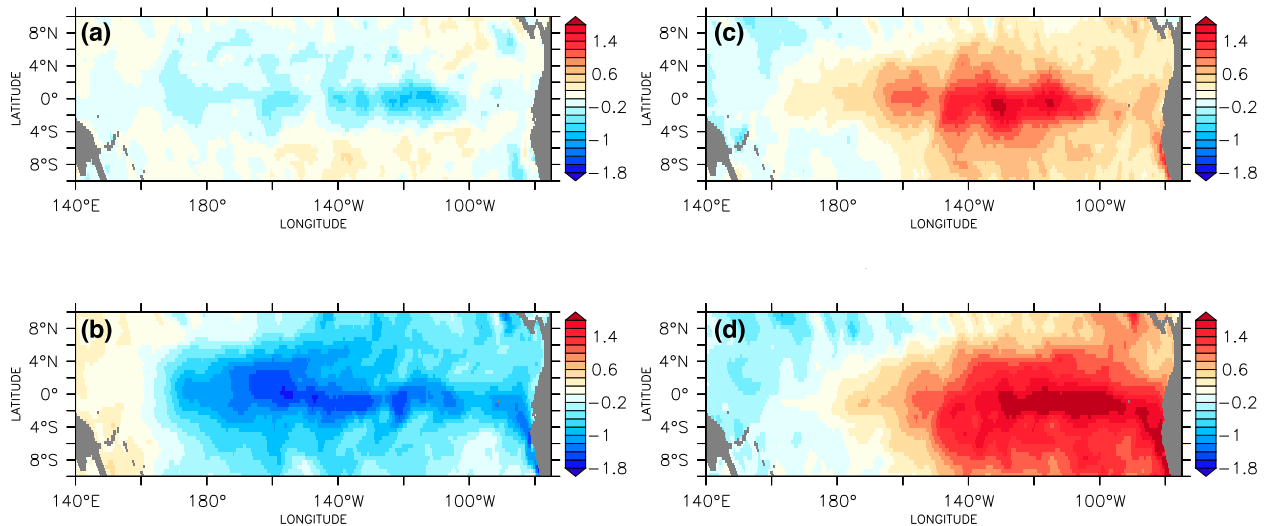


FIG. 13. Composites of DJF Pacific SST ($^{\circ}\text{C}$) anomalies from SODA in the year (top) preceding and (bottom) following (a),(b) warm and (c),(d) cold strong connection years.

We have explored the roles of ocean adjustment via Rossby and Kelvin wave propagation, meridional advection of subsurface temperature anomalies, and intra-seasonal wind stress variations as possible mechanisms by which the SAA-induced variations in the wind power impact SST in the eastern equatorial Atlantic. From our analysis, it appears that all of these mechanisms contribute to varying degrees in different years.

While there is a significant correlation between anomalies of SAA and wind power, wind power and SST, and ultimately SAA and SST, not every SAA anomaly is followed by a warming or cooling in the eastern equatorial Atlantic. In some years, the effect of the SAA strength on the tropical Atlantic wind power appears to be overridden by local effects in the near equatorial band, with an SAA anomaly not resulting in anomalous tropical Atlantic wind power.

It is noteworthy that the relationship among the SAA, tropical Atlantic wind power, and EEA SST might not be obvious when analyzing time series of all calendar months. In addition to the pronounced seasonal phase locking that requires a monthly stratified analysis, the situation is further complicated by the difference in timing between cold and warm years.

Understanding the drivers of interannual SST variability in the eastern equatorial Atlantic is of critical importance because of its connection to rainfall variability over western Africa. The results of our study, emphasizing the importance of remote forcing from the south through variations in the South Atlantic anticyclone, contributes to our knowledge of the connections between the tropical and subtropical Atlantic on interannual time scales as a step toward a more complete

understanding of climate variability of great societal relevance in this region.

Acknowledgments. This research was performed while the first author held a National Research Council Research Associateship Award at NOAA/PMEL. The constructive comments from three anonymous reviewers are greatly acknowledged.

REFERENCES

- Behringer, D., and Y. Xue, 2004: Evaluation of the global ocean data assimilation system at NCEP: The Pacific Ocean. Preprints, *Eighth Symp. on Integrated Observing and Assimilation Systems for Atmosphere, Oceans, and Land Surface*, Seattle, WA, Amer. Meteor. Soc., 2.3. [Available online at <https://ams.confex.com/ams/pdfpapers/70720.pdf>.]
- Brandt, P., and Coauthors, 2011: Equatorial upper-ocean dynamics and their interaction with the West African monsoon. *Atmos. Sci. Lett.*, **12**, 24–30, doi:10.1002/asl.287.
- Brown, J. N., and A. V. Fedorov, 2010: How much energy is transferred from the winds to the thermocline on ENSO timescales? *J. Climate*, **23**, 1563–1580, doi:10.1175/2009JCLI2914.1.
- Burls, N. J., C. J. C. Reason, P. Penven, and S. G. Philander, 2011: Similarities between the tropical Atlantic seasonal cycle and ENSO: An energetics perspective. *J. Geophys. Res.*, **116**, C11010, doi:10.1029/2011JC007164.
- , —, —, and —, 2012: Energetics of the tropical Atlantic zonal mode. *J. Climate*, **25**, 7442–7466, doi:10.1175/JCLI-D-11-00602.1.
- Caniaux, G., H. Giordani, J.-L. Redelsperger, F. Guichard, E. Key, and M. Wade, 2011: Coupling between the Atlantic cold tongue and the West African monsoon in boreal spring and summer. *J. Geophys. Res.*, **116**, C04003, doi:10.1029/2010JC006570.
- Carton, J., and B. S. Giese, 2008: A reanalysis of ocean climate using Simple Ocean Data Assimilation (SODA). *Mon. Wea. Rev.*, **136**, 2999–3017, doi:10.1175/2007MWR1978.1.

- Colberg, F., C. J. C. Reason, and K. Rodgers, 2004: South Atlantic response to El Niño–Southern Oscillation induced climate variability in an ocean general circulation model. *J. Geophys. Res.*, **109**, C12015, doi:10.1029/2004JC002301.
- Compo, G. P., and Coauthors, 2011: The Twentieth Century Reanalysis Project. *Quart. J. Roy. Meteor. Soc.*, **137**, 1–28, doi:10.1002/qj.776.
- Dee, D. P., and Coauthors, 2011: The ERA-Interim reanalysis: Configuration and performance of the data assimilation system. *Quart. J. Roy. Meteor. Soc.*, **137**, 553–597, doi:10.1002/qj.828.
- Ding, H., N. S. Keenlyside, and M. Latif, 2009: Seasonal cycle in the upper equatorial Atlantic Ocean. *J. Geophys. Res.*, **114**, C09016, doi:10.1029/2009JC005418.
- , —, and —, 2011: Impact of the equatorial Atlantic on the El Niño Southern Oscillation. *Climate Dyn.*, **38**, 1965–1972, doi:10.1007/s00382-011-1097-y.
- Fedorov, A. V., 2007: Net energy dissipation rates in the tropical ocean and ENSO dynamics. *J. Climate*, **20**, 1108–1117, doi:10.1175/JCLI4024.1.
- , S. L. Harper, S. G. H. Philander, B. Winter, and A. Wittenberg, 2003: How predictable is El Niño? *Bull. Amer. Meteor. Soc.*, **84**, 911–919, doi:10.1175/BAMS-84-7-911.
- Foltz, G. R., and M. J. McPhaden, 2010: Interaction between the Atlantic meridional and Niño modes. *Geophys. Res. Lett.*, **37**, L18604, doi:10.1029/2010GL044001.
- Frankignoul, C., and K. Hasselmann, 1977: Stochastic climate models. Part II: Application to SST anomalies and thermocline variability. *Tellus*, **29**, 289–305, doi:10.1111/j.2153-3490.1977.tb00740.x.
- Goddard, L., and S. G. H. Philander, 2000: The energetics of El Niño and La Niña. *J. Climate*, **13**, 1496–1516, doi:10.1175/1520-0442(2000)013<1496:TEOENO>2.0.CO;2.
- Hu, Z., A. Kumar, B. Huang, and J. Zhu, 2013: Leading modes of the upper ocean temperature interannual variability along the equatorial Atlantic Ocean in NCEP GODAS. *J. Climate*, **26**, 4649–4663, doi:10.1175/JCLI-D-12-00629.1.
- Huang, B., 2004: Remotely forced variability in the tropical Atlantic Ocean. *Climate Dyn.*, **23**, 133–152, doi:10.1007/s00382-004-0443-8.
- , and J. Shukla, 2005: Ocean–atmosphere interactions in the tropical and subtropical Atlantic Ocean. *J. Climate*, **18**, 1652–1672, doi:10.1175/JCLI3368.1.
- Kanamitsu, M., W. Ebisuzaki, J. Woollen, S.-K. Yang, J. J. Hnilo, M. Fiorino, and G. L. Potter, 2002: NCEP–DOE AMIP-II Reanalysis (R-2). *Bull. Amer. Meteor. Soc.*, **83**, 1631–1643, doi:10.1175/BAMS-83-11-1631.
- Keenlyside, N. S., and M. Latif, 2007: Understanding equatorial Atlantic interannual variability. *J. Climate*, **20**, 131–142, doi:10.1175/JCLI3992.1.
- Lübbecke, J. F., and M. J. McPhaden, 2012: On the inconsistent relationship between Pacific and Atlantic Niños. *J. Climate*, **25**, 4294–4303, doi:10.1175/JCLI-D-11-00553.1.
- , C. W. Böning, N. S. Keenlyside, and S.-P. Xie, 2010: On the connection between Benguela and equatorial Atlantic Niños and the role of the South Atlantic anticyclone. *J. Geophys. Res.*, **115**, C09015, doi:10.1029/2009JC005964.
- Marin, F., G. Caniaux, H. Giordani, B. Bourlès, Y. Gouriou, and E. Key, 2009: Why were sea surface temperatures so different in the eastern equatorial Atlantic in June 2005 and 2006? *J. Phys. Oceanogr.*, **39**, 1416–1431, doi:10.1175/2008JPO4030.1.
- Mo, K. C., and S. Häkkinen, 2001: Interannual variability in the tropical Atlantic and linkages to the Pacific. *J. Climate*, **14**, 2740–2762, doi:10.1175/1520-0442(2001)014<2740:IVITTA>2.0.CO;2.
- Okumura, Y., and S.-P. Xie, 2006: Some overlooked features of tropical Atlantic climate leading to a new Niño-like phenomenon. *J. Climate*, **19**, 5859–5874, doi:10.1175/JCLI3928.1.
- Perez, R. C., V. Hormann, R. Lumpkin, P. Brandt, W. E. Johns, F. Hernandez, C. Schmid, and B. Bourles, 2013: Mean meridional currents in the central and eastern equatorial Atlantic. *Climate Dyn.*, doi:10.1007/s00382-013-1968-5.
- Richter, I., S. K. Behera, Y. Masumoto, B. Taguchi, N. Komori, and T. Yamagata, 2010: On the triggering of Benguela Niños: Remote equatorial versus local influences. *Geophys. Res. Lett.*, **37**, L20604, doi:10.1029/2010GL044461.
- , —, —, —, H. Sasaki, and T. Yamagata, 2013: Multiple causes of interannual sea surface temperature variability in the equatorial Atlantic Ocean. *Nat. Geosci.*, **6**, 43–47, doi:10.1038/ngeo1660.
- , S.-P. Xie, S. K. Behera, T. Doi, and Y. Masumoto, 2014: Equatorial Atlantic variability and its relation to mean state biases in CMIP5. *Climate Dyn.*, **42**, 171–188, doi:10.1007/s00382-012-1624-5.
- Rodriguez-Fonseca, B., I. Polo, J. Garcia-Serrano, T. Losada, E. Mohino, C. R. Mechoso, and F. Kucharski, 2009: Are Atlantic Niños enhancing Pacific ENSO events in recent decades? *Geophys. Res. Lett.*, **36**, L20705, doi:10.1029/2009GL040048.
- Scott, R. B., and Y. Xu, 2009: An update on the wind power input to the surface geostrophic flow of the World Ocean. *Deep-Sea Res. I*, **56**, 295–304, doi:10.1016/j.dsr.2008.09.010.
- Sterl, A., and W. Hazeleger, 2003: Coupled variability and air–sea interaction in the South Atlantic Ocean. *Climate Dyn.*, **21**, 559–571, doi:10.1007/s00382-003-0348-y.